MODELING OF GROUNDWATER FLOW AND TCE TRANSPORT IN THE VALCARTIER AREA AQUIFER SYSTEM

Alexandre Boutin, Institut national de la recherche scientifique, INRS-Eau, Terre et Environnement, Québec
Now at TechnoRem Inc., Laval, Québec
René Lefebvre, Institut national de la recherche scientifique, INRS-Eau, Terre et Environnement, Québec
Véronique Blais, Institut national de la recherche scientifique, INRS-Eau, Terre et Environnement, Québec
Richard Martel, Institut national de la recherche scientifique, INRS-Eau, Terre et Environnement, Québec
René Therrien, Laval University, Geology and Geological Engineering Department, Québec
Michel Parent, Natural Resources Canada, Geological Survey of Canada, Québec

ABSTRACT
Numerical modeling using FRAC3DVS was used to understand groundwater flow and contaminant transport in a complex granular aquifer system contaminated by dissolved 1,1,2-trichloroethene (TCE) and daughter products. A 3D finite-element grid was built to represent the hydrostratigraphic context of the region comprising four units. The grid includes 30 layers and over a million elements. The numerical model was able to correctly represent the observed complex groundwater flow. TCE transport modeling was done to verify if the five suspected contaminant source zones could produce a TCE plume similar to the observed one. Transport modeling was also used to evaluate the relative contribution of the contaminant sources on the impacted receptors. Transport simulations correctly reproduced the morphology of the regional groundwater plume and allowed estimation of migration time from each source to the receptors. The results of this groundwater flow and transport modeling study enhanced the understanding of the different mechanisms controlling the migration of the regional TCE plume in groundwater.

RÉSUMÉ
Une modélisation numérique utilisant FRAC3DVS a été réalisée pour comprendre l'écoulement et le transport de contaminant dans un système aquifère granulaire complexe contaminé par du trichloro-1,1,2-éthène (TCE) dissous et ses produits de dégradation. Un maillage 3D en éléments finis a été construit afin de représenter le contexte hydrostratigraphique du secteur comprenant quatre unités. Le maillage comprend 30 couches et plus d'un million d'éléments. Le modèle a bien représenté les conditions complexes d'écoulement observées. Les simulations du transport ont permis de vérifier si les sources suspectées peuvent produire un panache de contamination comparable à celui observé. Aussi, le transport de masse sert à définir la contribution respective des principales zones sources à la contamination de milieux récepteurs. Les simulations du transport de masse ont aussi permis de quantifier le temps de migration à partir des différentes sources potentielles. Les résultats des simulations de l'écoulement et du transport de masse ont permis de comprendre les mécanismes ayant formés le panache de TCE d'envergure régionale.

1. INTRODUCTION

This paper presents a groundwater modeling study related to the contamination of a granular aquifer located in the Valcartier area, 35 km north of downtown Québec City, Canada. A companion paper by Lefebvre et al. (2004) describes the characterization program carried out to define the hydrogeological context and delineate the large dissolved TCE plume in groundwater. Because of both the complexity and the numerous data available, a detailed groundwater modeling study was realized to better understand the processes controlling groundwater flow and TCE migration in the Valcartier area (Boutin, 2004; Lefebvre et al. 2003).

Figure 1 presents the general context of the study area. It is mostly flat and bounded to the west by the Jacques-Cartier River and to the east by the Nelson River. Large hills (Brillant and Rolland-Auger) lie east and south of the Valcartier Garrison. Municipal and private wells use groundwater as a drinking water supply at each end of the study area and the Valcartier Garrison also uses wells for its water supply.

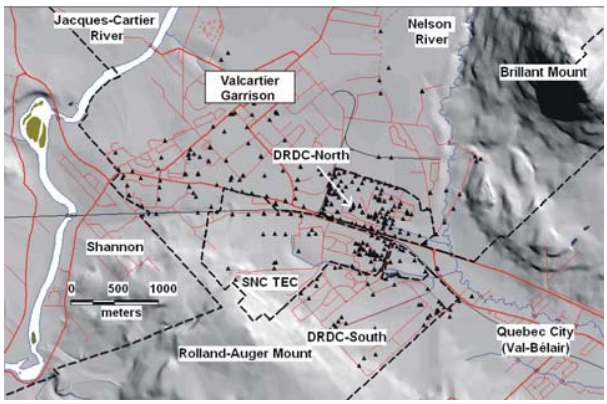

Figure 1. General context of the study area

2. OBJECTIVES

The objectives of the groundwater flow and mass transport modeling study were the following:

1. To represent hydrostratigraphic units by developing a complete and representative conceptual model for both groundwater flow and mass transport;
2. To simulate complex groundwater flow and represent key features of the flow regime that are directly controlling the dissolved TCE migration such as the position of the groundwater divide, vertical hydraulic gradients across the semi-confining silty unit and groundwater velocities;
3. Using mass transport modeling, to simulate TCE migration to determine if the suspected source zones can generate a dissolved TCE plume with a similar morphology. Also evaluate the time of travel needed for the contaminant migration from each of the sources to the receptors.

3. CONCEPTUAL MODEL AND GRID DESIGN

3.1 Selection of the groundwater modeling code

FRAC3DVS was developed for the simulation of groundwater flow and mass transport in discretely fractured rock aquifers (Therrien and Sudicky, 1996). The model can also simulate both saturated and unsaturated groundwater flow in porous media. The unsaturated flow is represented in the model using Richard's equation (Cooley, 1983; Huyakorn et al., 1984):

$$\frac{\partial}{\partial x_i}\left(K_{ij}k_{rw}\frac{\partial(\psi+z)}{\partial x_j}\right)\pm Q=\frac{\partial}{\partial t}(\theta_s S_w), i, j=1,2,3$$

To solve Richard's equation, FRAC3DVS uses the finite-element control volume method (Forsyth et Kropinski, 1997; Forsyth, 1991). This method allows the solution of the equation by iteration using the Newton-Raphson approach (Forsyth and Simpson, 1991). The ORTHOMIN solver is used to solve the linear equations matrix.

The Groundwater Modeling System (GMS) was used as a pre-processor and grid builder (BYU, 2000). Boundary conditions were assigned in GMS and FRAC3DVS can read files directly from GMS. The visualisation software TECPLOT (Amtec Engineering Inc., 2001) was used for post processing of the data and to explore and efficiently evaluate the numerous simulation results. Particle tracking is also possible in TECPLOT, directly using the output files generated by FRAC3DVS.

3.2 Groundwater flow conceptual model

The development of the conceptual model comprised the usual steps (Anderson and Woessner, 1992):

1. Choose model domain and boundary conditions;
2. Define hydrostratigraphic units;
3. Evaluate the water budget;
4. Define the flow system.

The simulations were completed under steady-state conditions. Saturated as well as unsaturated groundwater flow is represented in the model.

3.2.1 Model extent, boundary conditions and units

Figure 2 present the 2D grid and the boundary flow conditions. The modeling domain is located between the Jacques Cartier River to the west and Mount Brillant to the east. It is bounded to the south by Rolland-Auger mount and, to the north, the model ends at a distance of about 2 km north of the DRDC-North property limit. The total area of the model is approximately 12.5 km^2. The 2D grid extends 4.5 km from west to east and 3.3 km from south to north. The grid is refined at water supply wells, at the border of the prodeltaic silty unit characterized by a sharp hydraulic gradient and also within the limits of the TCE plume.

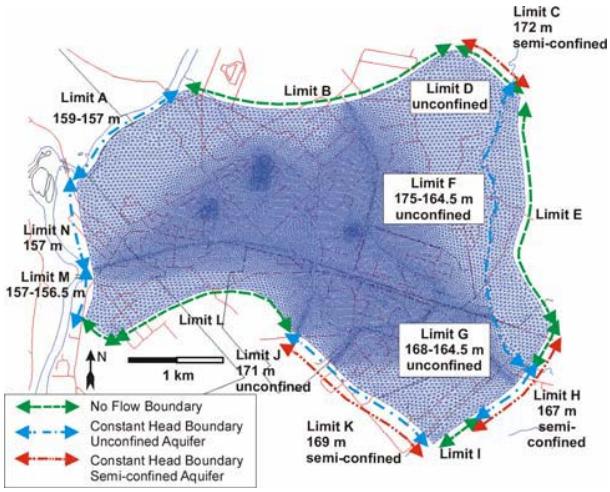

Figure 2. Modeling domain, 2D grid and boundary condition at the limits of the model

To represent complex groundwater flow within the aquifer system, different types of boundary conditions were assigned (Figure 2). No-flow and constant head boundary conditions were assigned around the 3D grid. These boundary conditions are based on the piezometric map built during the hydrogeological characterization of the aquifer system (Lefebvre et al., 2004, Boutin, 2004, Lefebvre et al., 2003, Boutin et al., 2002, Martel et al., 2000, Michaud et al., 1999). The major hydrostratigraphic units included in the model, from bottom to top are: proglacial sand and gravel, glaciomarine massive silts, prodeltaic silts, and deltaic sands (Lefebvre et al., 2004; Boutin, 2004; Lefebvre et al. 2003). The deltaic sand is divided into lower and upper parts (under and above the prodeltaic silts where present). A total of 16 hydraulic conductivity *K* zones were created to represent the variation of *K* within this hydrostragraphic unit. Figure 3 shows the distribution of the *K* zones in the deltaic unit.

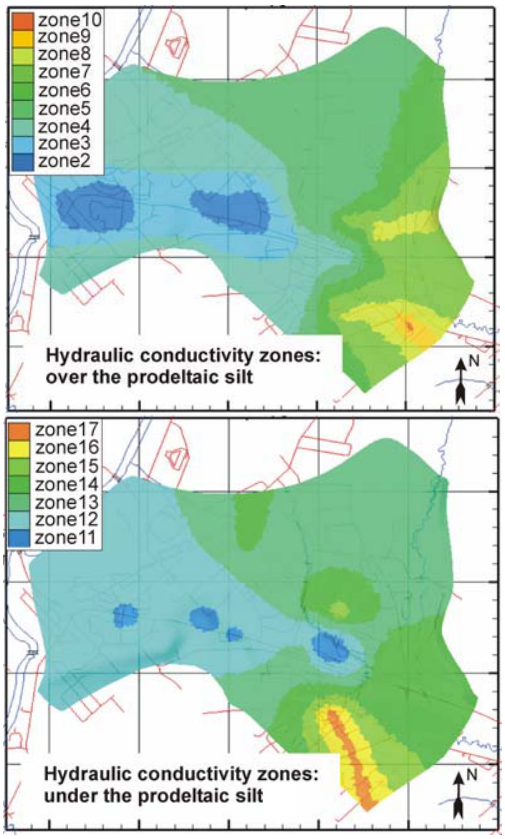

Figure 3. Location of the hydraulic conductivity zones within the deltaic sands unit

3.2.2 3D finite-element grid

To avoid convergence problems and to assign precise hydraulic properties, hydraulic heads and contaminant concentrations, a detailed vertical discretization was assigned to the grid. A total of 30 layers are included in the 3D grid. Table 1 shows the distribution of the layers for each of the hydrostratigraphic units. Figure 4 presents a 3D view of the grid and an east-west section. The 3D grid contains 1 067 040 elements (35 568 per layer).

Table 1. Layers assigned in the 3D model for each unit.

Units	No. of layers
Deltaic Sands	24 (18)
Prodeltaic Silts	(6)
Glaciomarine Silts	2
Proglacial Sand and Gravel	4
Total	30

( ) number of layers when prodeltaic silt splits the deltaic sand

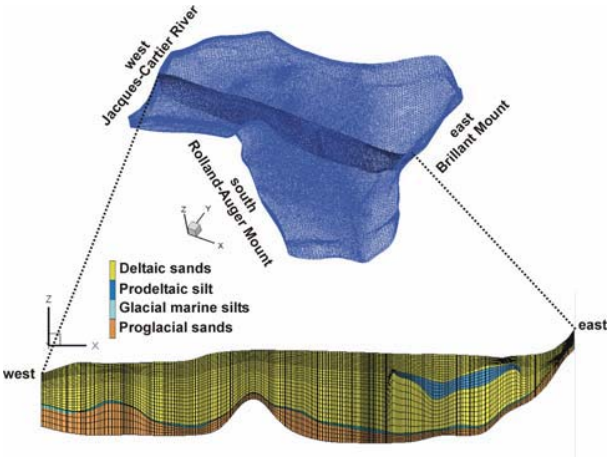

Figure 4. General view of the 3D finite-element grid and east-west section of the grid showing hydrostratigraphic units and vertical discretization

3.3 Dissolved TCE transport conceptual model

The detailed characterization work performed to understand the distribution of dissolved TCE in groundwater identified five (5) suspected TCE source zones (Lefebvre et al., 2004; Boutin, 2004; Lefebvre et al., 2003). These were all included in the dissolved TCE transport conceptual model. Fixed concentrations were assigned to the nodes at these source zones. The concentration value assigned is 50 000 µg/L which is representative of the highest concentration historically measured at the site. In the transport model, all sources were set active at time 0 and emitted contaminant for the whole duration of the simulations (60 years). Figure 5 locates the five (5) dissolved TCE suspected sources assigned to carry out the TCE mass transport simulation.

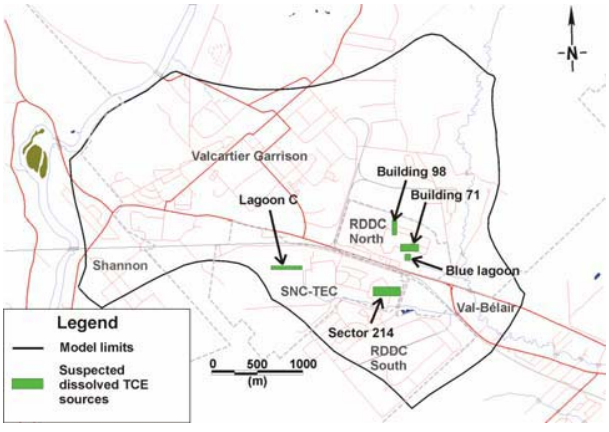

Figure 5. Location of the imposed concentration source zones in the dissolved TCE transport simulations

Two other constant concentration boundary conditions were assigned in the model. A specified zero concentration condition was assigned at top surface, as well as at the south-western (Rolland-Auger Mount) and north-eastern limits of the model. These two specified null concentration boundary conditions were assigned to avoid introduction of negative concentrations while computing upstream concentration values (Zheng and Bennett, 2002).

4. MODEL CALIBRATION AND VERIFICATION

4.1 Calibration Process and Model Error

Model calibration was achieved by trial and error. Hydraulic conductivities and groundwater recharge were modified to reach calibration. Changes to the constant head boundary values were also necessary to correctly represent groundwater flow characteristics. The calibration target was set to 5% of the simulated hydraulic head distribution, which is 0.925 m (175 m – 156.5 m = 18.5 m; 18.5 m × 5%) (Anderson and Woessner, 1992).

A total of 582 measured hydraulic heads were used to quantify the error distribution of the model. The hydraulic heads field data are distributed in both unconfined and semi-confined aquifers. Figure 6 shows the simulated and observed heads. The graph shows that the calibration is reached but that some error still remains for the observed hydraulic head values, ranging from 160 m to 165 m measured in the western part of the site. The eastern part of the site shows a better correlation between the simulated and the measured hydraulic heads.

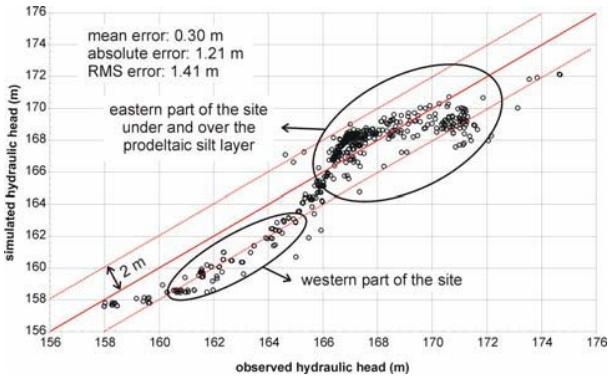

Figure 6. Simulated and observed hydraulic heads

The mean error of the calibrated model is 0.30 m, the absolute error 1.21 m and the RMS (root mean square) error is 1.41 m. The calibration target (0.925) is not entirely reached but the calibration is considered completed.

The set of parameters (hydraulic conductivity and recharge) that were assigned to calibrate the model are presented in Table 2. Horizontal hydraulic conductivities range from $1.0x10^{-7}$ m/s to $3.0x10^{-4}$ m/s. The calibrated value of groundwater recharge is 350 mm/yr.

Table 2. Parameters assigned to the calibrated groundwater flow numerical model.

Hydrostratigraphic units	Zone in the model	$K_x = K_y$ (m/s)	K_z (m/s)
Proglacial	1	$3.0x10^{-4}$	$3.0x10^{-5}$
Upper deltaic	2	$8.0x10^{-5}$	$8.0x10^{-6}$
	3	$6.0x10^{-5}$	$6.0x10^{-6}$
	4	$4.0x10^{-5}$	$4.0x10^{-6}$
	5	$1.0x10^{-5}$	$1.0x10^{-6}$
	6	$9.0x10^{-6}$	$9.0x10^{-7}$
	7	$7.0x10^{-6}$	$7.0x10^{-7}$
	8	$5.0x10^{-6}$	$5.0x10^{-7}$
	9	$4.0x10^{-6}$	$4.0x10^{-7}$
	10	$3.0x10^{-6}$	$3.0x10^{-7}$
Lower deltaic	11	$3.0x10^{-4}$	$3.0x10^{-5}$
	12	$1.5x10^{-4}$	$1.5x10^{-5}$
	13	$1.1x10^{-4}$	$1.1x10^{-5}$
	14	$1.3x10^{-4}$	$1.3x10^{-5}$
	15	$7.9x10^{-5}$	$7.9x10^{-6}$
	16	$5.0x10^{-5}$	$5.0x10^{-6}$
	17	$3.1x10^{-5}$	$3.1x10^{-6}$
Prodeltaic silts	18	$1.0x10^{-7}$	$1.0x10^{-8}$
Glaciomarine silts	19	$5.0x10^{-5}$	$5.0x10^{-6}$
-	Recharge (mm/yr)	350	

Both saturated and unsaturated flow is simulated with the Valcartier groundwater flow model. During calibration, the van Genuchten (1980) capillary parameters were adjusted to allow convergence of the simulations and the correct representation of the unsaturated zone. Table 3 presents a summary of the capillarity parameters assigned to the calibrated model. A compilation of typical parameters was used to assign the parameters (Carsel and Parrish, 1988).

Table 3. Capillarity parameters assigned to the calibrated groundwater flow model.

Unit	Porosity	S_{wr}	α	β	γ	Air entry pressure (m)
Deltaic sand	0.33	0.12	14.5	2	0.35	-0.35
Glacial marine silts	Tabulated values					
Prodeltaic silts	Tabulated values					

4.2 Sensitivity analysis of the calibrated model

A complete sensitivity study of the calibrated model was carried out to check if the set of parameters assigned to the model were minimising the error. Independently varying the hydraulic conductivities and the groundwater recharge was done for the sensitivity study. The hydraulic conductivities were lowered and increased by 10%, 20%, 30% and 40%. Besides the calibrated value of 350 mm/yr, five (5) other values of recharge were assigned to the model: 200, 250, 300, 400 and 450 mm/yr. Figure 7 presents the error for each of the simulation runs performed for the sensitivity analysis. The sensitivity analysis results clearly demonstrate that the calibrated model minimizes the mean, absolute and RMS errors.

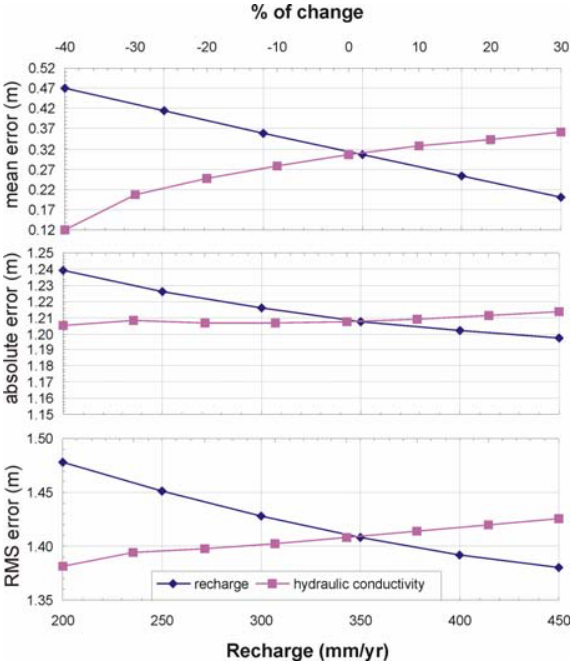

Figure 7. Sensitivity of the calibrated model to changes in groundwater recharge and hydraulic conductivity

Another sensitivity analysis was made by modifying the specified head values imposed as boundary conditions around the 3D grid (Boutin, 2004; Lefebvre et al., 2003). This second analysis indicated that the error is not always minimised by some changes in specified head at the boundary of the model. The model calibration was carried by trying first to minimize the error between simulated and measured hydraulic heads, as is commonly done (Anderson and Woessner, 1992). However, the model calibration also tried to reproduce the location of the groundwater divide that is critical to properly represent TCE mass transport from some source zones. This explains why some combinations of specified head at the limits could lead to smaller error values. However, for these cases the position of the groundwater divide did not correspond to the observed position (Boutin, 2004).

4.3 Regional distribution of the simulated errors

Before concluding that the groundwater model is calibrated it is important to verify if the error distribution on the site is sparse or concentrated in some areas. Mapping the error is useful to visually verify any trends in the data. Figure 8 shows the error distribution at each of the measurement points. It shows that generally the error is well distributed except for some high values concentrated at the western part of the site. This could be explained by the absence in this area of the glaciomarine silt unit under the deltaic sand that could not be represented well in the model due to a lack of data. For this reason, it was difficult to correctly simulate the observed hydraulic heads in this area of the site while maintaining a small error in the eastern part of the study area. It was judged important to represent the eastern part of the model more precisely as it is where most of the source zones are located (Sector 214 and three suspected sources within DRDC-North).

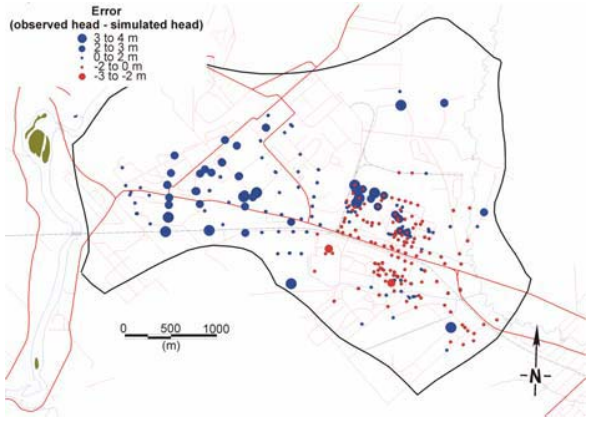

Figure 8. Error distribution in hydraulic head of the calibrated groundwater flow model

The centre of the site also shows some higher error in simulated heads. These errors are located at the border of the prodeltaic silty unit that is absent in the western part of the study area. A sharp hydraulic gradient is measured at the border of the prodeltaic silty layer, and the model did not precisely represent this special feature of the groundwater flow system.

The model calibration process also involved a verification that the model correctly simulates the high vertical hydraulic gradient observed between the unconfined aquifer above the prodeltaic silty unit and the semi-confined aquifer under that silty layer. The value of the vertical hydraulic conductivity of the material in the prodeltaic silty unit was key in obtaining a vertical hydraulic gradient across this unit. The calibrated model correctly simulates this gradient that controls transport of dissolved TCE for the sources above the silty unit in this area, as groundwater tends to flow downward through the prodeltaic silty layer (Lefebvre et al., 2004).

5. GROUNDWATER FLOW MODELING RESULTS

5.1 Simulated hydraulic head distribution

Figure 9 (top) presents the simulated hydraulic heads over the entire modeling domain. It shows the crescent-shaped hydraulic head distribution. The horizontal hydraulic gradients simulated by the model are similar to those observed in the field (Lefebvre et al., 2004). The dotted lines on the figure locate the vertical sections shown on Figures 9 and 10.

Dissolved TCE transport is controlled by vertical hydraulic gradient across the prodeltaic silty layer for the suspected TCE sources located within DRDC-North. As illustrated on the section presented in Figure 9 (bottom), the model correctly represents the vertical gradient across the prodeltaic silty layer.

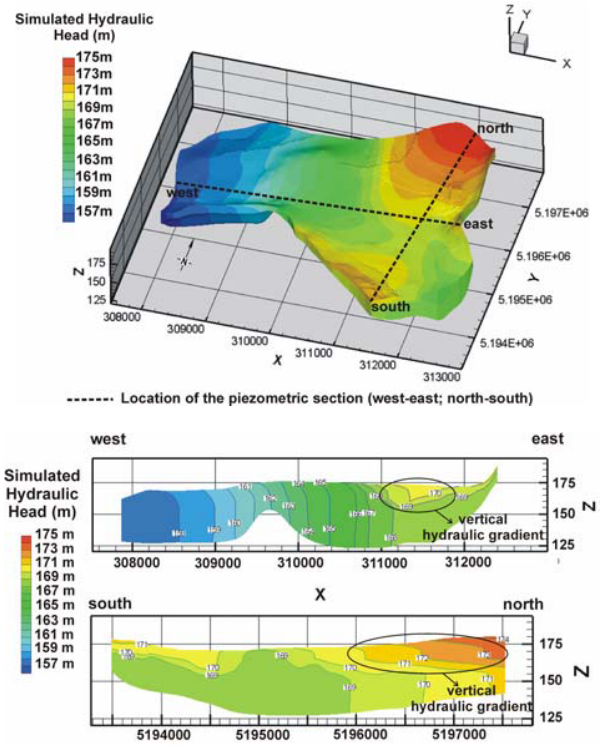

Figure 9. 3D view of the simulated hydraulic head (top) and vertical sections showing hydraulic head (bottom)

5.2 Simulated water saturation distribution

The model simulates saturated and unsaturated groundwater flow and thus calculates the distribution of water saturation in the aquifer. Figure 10 shows vertical cross-sections of the simulated water saturation (location on Figure 9). Water saturation varies between the residual water saturation fixed at 0.12 and complete water saturation under the water table. Figure 10 shows that the thickness of the unsaturated zone varies from less than a meter close to the groundwater divide to the east of the site to more than 10 m in the western part.

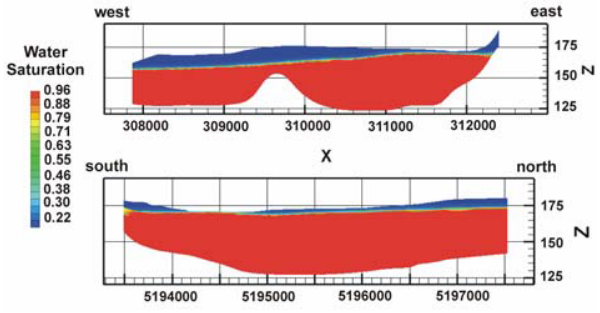

Figure 10. Cross-sections showing the simulated water saturation (location of cross-sections shown on Figure 9)

5.3 Particle tracking

Particle tracking was used in the groundwater flow model to determine the zones of contribution of supply wells and to determine the time of travel from the suspected source zones to the receptors. Figure 11 shows the simulated zones of contribution of four wells within the Valcartier Garrison. Well P-5, where the TCE contamination was first detected, is seen to be within the TCE plume. Well P-2 is at the edge of the plume and its alert wells have detected TCE already. Wells P-5 and P-2 are no longer used for water supply. The zones of contribution of well P-4 and the new well P-7 are outside of the plume.

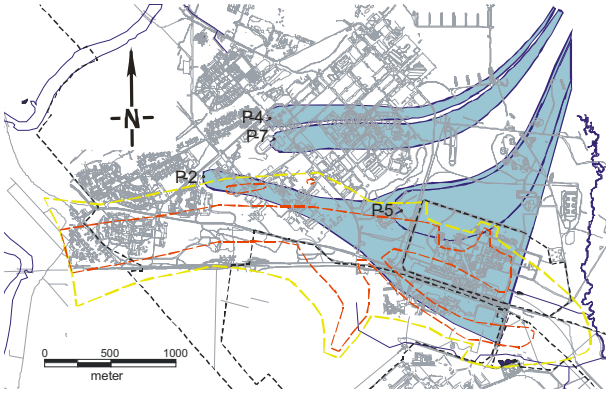

Figure 11. Simulated zones of contribution of wells in relation with the observed extent of the TCE plume (the yellow line delineates where TCE is detected and the red line the area where TCE concentration exceeds 50 μg/L)

Figure 12 illustrates the results of particle tracking used to estimate the time of travel from source zones to receptors. Particles were released in the deltaic sand aquifer under the prodeltaic silty unit where it is present.

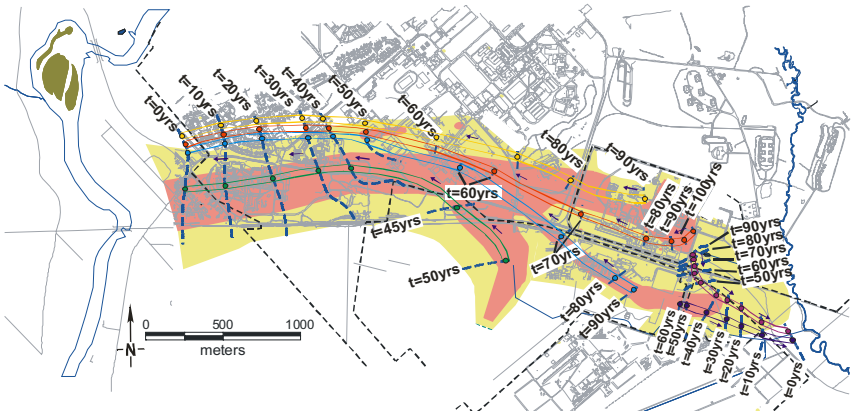

Figure 12. Time of travel from source zones to receptors obtained with particle tracking in the groundwater flow model

Figure 12 shows the time of travel in the upstream direction, i.e. from the receptors in the opposite direction of groundwater flow. This representation better evaluates the possibility that a source zone can be related to the contamination of the receptors and also relates different parts of the plume to different source zones. Figure 12 shows that groundwater velocity is slow in the eastern part of the site. The longer migration times for the suspected sources that are close to the groundwater divide are explained by the small hydraulic gradient and also the generally lower hydraulic conductivity of the materials is in that area. The groundwater flow is faster in the western part of the site.

6. TCE TRANSPORT MODELING RESULTS

6.1 Calibrated transport parameters

The transport model was calibrated by comparing the 2D distribution of the observed and simulated plume. The objective of the transport simulation was not to represent perfectly the concentrations distribution in the 3D contaminated groundwater plume. Based on column tests and the distribution of TCE daughter products in the TCE plume, the transport simulations were performed without retardation and biodegradation. The calibrated horizontal dispersivity coefficient α_x is 10 m, horizontal transverse dispersivity α_y is 0.01 m and vertical transverse dispersivity coefficient α_z is 0.001 m. Simulation of TCE migration in the aquifer system was made for 60 years, which is the maximum estimated emission time for the suspected source zones. In the model, all sources were supposed active for the entire duration of the simulations, from time 0 to 60 years. No historic data were available to assign more specific source terms.

6.2 Simulated TCE distribution

Figure 13 shows the simulated dissolved TCE plume after 25 and 60 years of migration. It can be observed for the 60 years simulation that the morphology of the simulated and observed (dotted lines, Lefebvre et al., 2004) dissolved TCE plume is similar. As observed, the eastern source zones of the model (B-98, B71, East Fence and Sector 214) emit dissolved TCE to the east and to the west. These sources are located at the groundwater divide in the unconfined and semi-confined aquifer (Lefebvre et al., 2004). Figure 13 shows that the TCE plume emitted from the eastern source zones of the model tends to coalesce and have a restricted width away from the sources. The increased groundwater velocity away from these source zones induces a reduction of the flow area needed to transport the TCE away from the sources. Thus, this is an interesting case where the plume width is reduced away from the source due to the focussing of the groundwater flow rather than increasing in width due to dispersion. On the contrary, a local high in the bedrock topography is seen to cause the radial spreading of TCE originating from the Lagoon C source zone, thus forming a plume exceeding 600 m in width away from this source zone.

7. CONCLUSIONS

The development of a detailed groundwater flow and mass transport numerical model allowed the representation of the complex flow system and provides and explanation for the transport of dissolved TCE in the Valcartier area. The model was first able to represent the complex groundwater flow involving a partly saturated system with high vertical hydraulic gradients, a groundwater divide, and varying groundwater flow velocities. Transport simulations were able to represent the general morphology of the observed dissolved TCE groundwater plume and the relationships between the suspected sources and the plume. The model will also served to plan future control and rehabilitation actions.

8. ACKNOWLEDGMENTS

The DND supported this research and granted permission to publish. Thanks to DND personnel: Michael Hodgson, Mireille Lapointe, Stéphane Jean and Nathalie Roy. Thanks to other organizations for data: Shannon, Québec City, SNC-TEC, and MENVQ. R.L., R.M. and R.T. acknowledge NSERC and NATEQ grants.

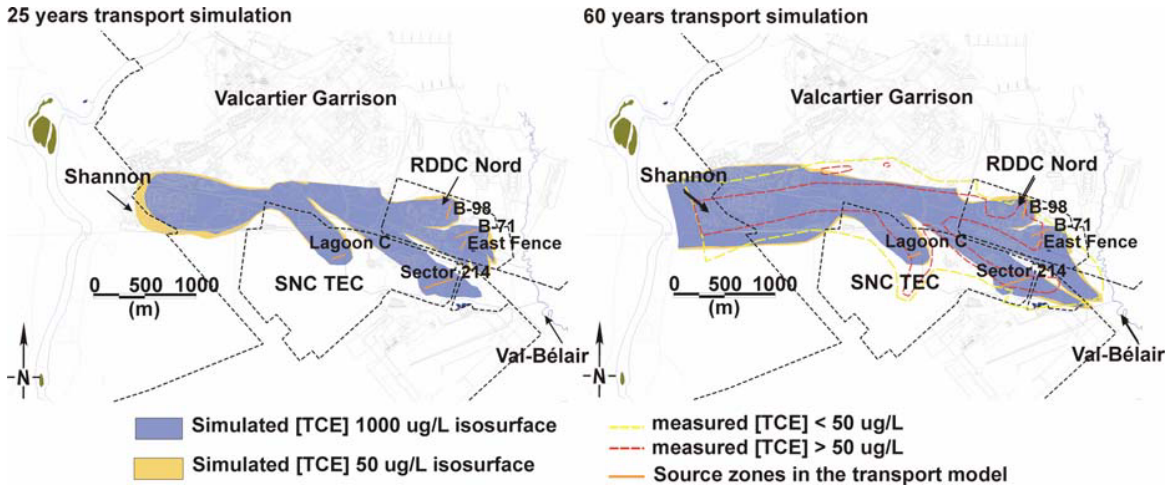

Figure 13. Two-dimensional simulated dissolved TCE plume after 25 years and 60 years of simulation

9. REFERENCES

Amtec Engineering, Inc., 2001. Tecplot User's Manual, Version 9.0, 600 p.

Anderson, M.P., Woessner, W.W. 1992. Applied groundwater modeling: simulation of flow and advective transport. Academic Press, San Diego, 381 p.

Boutin, A., 2004. *Caractérisation et modélisation numérique de la contamination en TCE dans l'eau souterraine du secteur Valcartier, Québec, Canada* [In French]. M.Sc. Thesis, INRS-ETE, January 2004.

Boutin, A., Lefebvre, R., Martel, R., Therrien, R., Parent, M., Paradis, D., 2002. Hydrogeological Mapping of a TCE plume in granulat aquifer, Valcartier, Quebec, Canada, 3rd Joint IAH-CNC and CGS Groundwater Specialty Conference, 55th Canadian Geotechnical Conference, Oct. 20-23, Niagara Falls, 1101-1108.

BYU, 2000. Department of Defense Groundwater Modeling System (GMS), Version 3.1, Tutorial Manual. Brigham Young University.

Carsel, R.F., Parrish, R.S. 1988. Developing joint probability distributions of soil water retention characteristics, Water Resources Research, vol. 24, no.5, p. 755-769.

Cooley, R.L., 1983. Some new procedures for numerical solution of variably saturated flow problems. Water Resour. Res., 19 (5), p. 1271-1285.

Forsyth, P.A., and Kropinski, M.C. 1997. Monotonicity considerations for saturated-unsaturated subsurface flow, SIAM Jounal of Scientific Computing, 18, 1328-1354.

Forsyth, P.A., 1991. A control volume finite element approach to NAPL groundwater contamination. J. Sci. Stat. Comput., 12 (5), p. 1029-1057.

Forsyth, P.A., Simpson, R.B., 1991. A two phase, two component model for natural convection in a porous medium. Int. J. Num. Meth. Fluids, 12, p. 655-682.

Huyakorn, P.S., Thomas, S.D., Thompson, B.M., 1984. Techniques for making finite elements competitive in modeling flow in variably saturated porous media. Water Resour. Res., 19 (4), p. 1019-1035.

Lefebvre, R., Boutin, A., Blais, V., Parent, M, Ouellon, T., Martel, R., Therrien, R., Roy, N., Lapointe, M., 2004. Hydrogeological Context and Dissolved TCE Plume Characterization in the Valcartier Area, Quebec, Canada, 5th Joint IAH-CNC and CGS Groundwater Specialty Conference, 57th Canadian Geotechnical Conference, Oct. 24-27, 2004, Quebec, Canada, 8p.

Lefebvre, R., Boutin, A., Martel, R., Therrien, R., Parent, M., Blais, V., 2003. *Caractérisation et modélisation numérique de l'écoulement et de la migration de la contamination en TCE dans l'eau souterraine du secteur Valcartier, Québec, Canada* [In French]. INRS-ETE R-631, mai 2003, 99 p., 28 planches et annexes. http://www.inrs-ete.uquebec.ca/publications/epub.htm

Martel, R., Parent, M., Lefebvre, R., Carrier, M-A., Paradis, D., Mailloux, M., Hardy, F., Michaud, Y., Boutin, A., 2000. *Caractérisation complémentaire des contextes géologique et hydrogéologique du secteur Valcartier*, [in french], 115 p.

Michaud, Y., Parent, M., Mailloux, M., Boisvert, É., Lefebvre, R., Martel, R., Boivin, R., Roy, N., Hains, S., 1999. *Cartographie des formations superficielles et cartographie hydrogéologique de la base des forces canadiennes Valcartier.*, [in french], Report submitted to the USS Valcartier, 1 CD-Rom, 2 maps.

Therrien, R., Sudicky, E.A. 1996. There dimensional analysis of variably saturated flow and solute transport in discretely-fractured porous media. J. of Contaminant Hydrology, 23, 1-44.

van Genuchten, M.Th., 1980. A closed-form equation for predicting the hydraulic conductivity of unsaturated soils. *Soil Sc. Soc. Am. J.*, 44, 892-898.

Zheng, C., Bennett, G.D., 2002. Applied Contaminant Transport Modeling 2nd ed. Wiley-Interscience, 621 p.